Atomic and Electronic Bulk versus Surface Structure: Lithium Intercalation in Anatase TiO_2

M. Wagemaker,[†] D. Lützenkirchen-Hecht,*[,‡] A. A. van Well,[†] and R. Frahm[‡]

Interfaculty Reactor Institute, Delft University of Technology, Mekelweg 15, 2629 JB Delft, The Netherlands, and Institut für Materialwissenschaften und Fachbereich C - Physik, Bergische Universität Wuppertal, Gaussstr. 20, 42097 Wuppertal, Germany

Received: April 1, 2004; In Final Form: June 18, 2004

Lithium intercalation in anatase TiO_2 results in structural and electronic changes. X-ray absorption at the Ti K edge as a function of lithium content is interpreted as a sum of two coexisting crystallographic phases (anatase and Li-titanate), both in the case of chemically lithiated microcrystalline samples and electrochemically intercalated thin film samples. The changes in the near edge region of the Ti K edge (XANES region) indicate that the charge-compensating electron of the Li-ion mainly occupies the crystal field split Ti *3d* t_{2g} orbitals located at the bottom of the conduction band. Surface sensitive reflection mode XAFS indicates that intercalation leads to a 3−4 nm surface region characterized by an effective Ti oxidation state close to 3+. The composition is determined to be close to Li_1TiO_2, and appears to be the reason for a poor cycle-lifetime of the anatase TiO_2 electrode material.

1. Introduction

Lithium intercalation in anatase TiO_2 is frequently studied for its applicability as electrode in rechargeable Li-ion batteries[1−3] and in electrochromic devices.[4,5] Lithium insertion results in a phase transition from the original tetragonal (space-group I_1/amd) anatase structure toward the orthorhombic $Li_{x\sim0.5}TiO_2$ phase (space-group *Imma*).[6] Throughout literature different Li fractions are reported for the orthorhombic phase, $x = 0.4$ up to $x = 1.0$, depending on the intercalation method, particle size and temperature.[6−12] At room temperature electrochemical intercalation appears to lead to values between $x = 0.4$ and 0.5, whereas chemical lithiation leads to slightly higher values, $x \sim 0.55$. Regardless of the exact composition we will refer to the $Li_{x=0.4-0.55}TiO_2$ phase as Li-titanate. During intercalation through thin film electrodes, the Li-titanate phase proceeds as a flat phase front parallel to the electrode surface.[8,13] The intercalation appears to be a self-limiting diffusion process preventing the phase transition to proceed through the whole TiO_2 anatase film or particle, depending on the dimensions.[8] In particular the phase front itself is suggested to limit the overall diffusion rate.[14,15] At elevated temperatures, anatase can be charged to the composition Li_1TiO_2, where all octahedral sites are filled.[12] However, this leads to poor reversibility of the intercalation.

Upon Li intercalation, the original white anatase powder turns dark blue and a thin film changes from transparent to partially reflecting. This electrochromic effect is most likely the result of the charge-compensating electrons that enter the material with the Li ions. It is generally assumed that in transition metal oxides the charge compensating electrons enter the lowest unoccupied bands mainly comprised of transition metal-3d orbitals that have a significant O-2p admixture.[16,17]

For anatase TiO_2, the coloration mechanism remains unclear, as different interpretations have been suggested. A number of authors attribute the electro-chromic effect to absorption by nearly free electrons, either compensating for the intercalated Li ions or for the Li ions accumulated at the solid/liquid interface.[18,19] This interpretation suggests a delocalized nature of the highest occupied electron states. In contrast, other authors suggest a semilocalized electron character based on conductivity and optical absorption[20,21] and polaron absorption of localized Ti^{3+} surface states.[22,23] More recently, the Ti^{3+} states in Li-inserted nanoporous anatase TiO_2 are directly related to the formation of the Li-rich phase (Li-titanate) rather then to surface states.[7] In bulk material, localized paramagnetic Ti^{3+}-3d states seem unlikely because they would lead to large chemical shifts in the ^{7}Li NMR spectra and prominent intensities in EPR spectra, both not observed in micro- and nanosized materials.[14,24,25] On the other hand, a localized character is suggested by the formation of covalent Ti−Ti bonds in lithium titanate (quenched electron orbital momentum) occupied by the charge compensating electrons.[20] More specifically, Nuspl et al.[26] argue that the structural change upon lithiation of anatase TiO_2 to Li-titanate can be explained by filling of the Ti-$3d_{yz}$ levels at the bottom of the conduction band. These Ti bands have a strong binding character with neighboring Ti atoms in the *yz* direction and as a result they form zigzag Ti−Ti bonds in this direction that stabilize the structure of Li titanate. A localized character of the electrons in the Ti−Ti zigzag bonds is consistent with the nonmetallic resistivity measured in Li-doped anatase,[21] which would not be expected if the electrons were delocalized over the whole Ti−O framework.[20]

The differences in the results reported in the literature concerning the electronic state of the charge compensating electrons could also be related to a difference in bulk and surface effects. With surface sensitive techniques localized Ti^{3+} states are consequently reported.[7,22,23]

1.1. Aim of this Study. The goal of this study is to establish a consistent picture of Li insertion in anatase TiO_2 within the framework of results that are present in the literature, and by presenting a systematic Ti K edge X-ray absorption (XAS)

* To whom correspondence should be addressed. E-mail: dirklh@uni-wuppertal.de.
[†] Delft University of Technology.
[‡] Bergische Universität Wuppertal.

10.1021/jp048567f CCC: $27.50
Published on Web 07/27/2004

study. Ti K edge XAS offers the possibility to study both the atomic structure (EXAFS) and the electronic structure (XANES). The aim here is to study the changes in the electronic state upon lithium insertion rather than the structural changes that are well-known[6,10,27] and in particular the difference in bulk and surface effects. As a result this study consists of two parts, transmission XAS of chemically lithiated anatase TiO_2 and quasi-in-situ reflection mode XAFS experiments on thin films of electrochemically lithiated anatase TiO_2. Transmission mode XAS is a bulk probe; that is, it cannot give any specific information about the surface structure of the sample. On the other hand, reflection mode grazing incidence XAS is a powerful tool to obtain structural and electronic information about the near surface region of electrochemically treated electrodes (see, e.g., refs 28−32). For grazing angles below the critical angle of total reflection, the X-ray penetration depth amounts to only a few nm;[33] therefore, the reflected signal only contains information about a very thin surface region of the specimen. This offers the unique opportunity to distinguish between bulk and surface effects related to the electrochromic effect. For the data interpretation, it is essential to realize that the XAS signal originates from two different crystallographic phases. In chemically lithiated micro powders, lithiation of anatase TiO_2 results in a lithium-poor anatase ($x \sim 0.01$) and a lithium-rich Li-titanate ($x \sim 0.55$) phase.[8,10,14] Neutron reflectometry revealed that Li intercalation in thin film anatase TiO_2 results in a smooth lithium-rich Li-titanate front penetrating the sample parallel to the film surface.[13] Hence, the reflecting XAS signal will originate from a two-layer system representing these two phases.

2. Materials and Methods

2.1. Sample Preparation. Microcrystalline anatase TiO_2 (99%) was obtained from Janssen Chimica. The Li_xTiO_2 samples were prepared by chemical intercalation of the pure powder with *n*-butyllithium (1.6 M from Aldrich).[11] The powders were mixed with hexane, and different amounts of *n*-butyllithium were added while stirring the mixture in order to obtain the following compositions of Li_xTiO_2: $x = 0.03$, 0.07, 0.12, 0.19, 0.25, 0.32, 0.41, 0.5, 0.6, and 0.7. All sample preparations were carried out in a glovebox in an inert argon atmosphere to prevent reaction of lithium with air or humidity. After preparation, the samples were subjected to wet-chemical inductively coupled plasma spectroscopy (ICP) analysis to check the overall composition, especially the Li/Ti ratio. These results confirmed that during preparation all of the lithium reacts with the anatase TiO_2, yielding the overall compositions with an accuracy of ±3% as calculated from the amount of *n*-butyllithium in the solution. The samples were thoroughly mixed with boron nitride to increase the powder volume (∼90 wt % boron nitride, ∼10 wt % Li_xTiO_2) so that mechanically stable samples could be pressed. Prior to the XAS measurements, transmission scans with a small pinhole across the sample were performed in order to check its homogeneity. The sample holders were sealed in a glovebox under argon atmosphere with Kapton windows to prevent sample degradation during the experiments.

Anatase TiO_2 thin films (∼25−30 nm thickness, 15 × 40 mm^2 width × length) were prepared by RF sputter deposition in a Perkin-Elmer 2400 system, further details can be found elsewhere.[13] Between the silicon substrate and the TiO_2 film, a gold film of 10−15 nm thickness serves as back contact for the electrochemical sample preparation. The lateral area of the TiO_2 film was slightly larger than that of the gold to prevent direct contact between the gold and the electrolyte.

2.2. X-ray Absorption Experiments. *2.2.1. General.* The experiments were performed at the X-ray undulator beamline BW1 at the DORIS III storage ring at Hasylab, (Hamburg, Germany) operating at a positron energy of 4.45 GeV with ∼100−150 mA of stored current. A double-crystal monochromator with two flat Si(111) crystals was used. More details about the beamline and the properties of the synchrotron radiation emitted by the X-ray undulator can be found in ref 34. Transmission XANES and EXAFS data were collected at the Ti K edge (∼4966 eV) at room temperature. In the vicinity of the absorption edge, it is assumed that the full width at half-maximum of all peaks in the derivative spectrum indicates the energy resolution of the instrument. We determined a value of 0.89 ± 0.05 eV (fwhm) from the 1st derivatives of measured XANES spectra of a Ti metal reference foil. Incident and transmitted intensities were measured with nitrogen-filled ionization chambers. A Ti metal foil was measured in transmission between the second and a third ionization chamber in order to calibrate the energy scale of the monochromator simultaneously with each of the samples. Suppression of higher harmonics in the Bragg-reflected beam was achieved by detuning the monochromator crystals to about 40−50% of the maximum intensity. Different crystalline Ti-reference compounds such as pure anatase and rutile TiO_2, $Li_{0.6}TiO_2$ (Li-titanate), $Li_4Ti_5O_{12}$ (Li−Ti-spinel), TiH_2, and different Ti-oxides (TiO, Ti_2O_3) were measured in transmission geometry for comparison.

2.2.2. Data Correction and Analysis. The XAS data analysis of the transmission mode spectra was performed using the WinXas program package.[35] The data reduction comprised a linear preedge background removal and data normalization. For the detailed analysis of the measured Ti K edge X-ray absorption of lithiated anatase, we also applied a principal component analysis (PCA),[36,37] which is also included in the WinXas package. With PCA, one can determine the minimal number and the type of the model compounds, which are necessary to reproduce the measured spectra by means of a linear combination.[38,39] More detailed, by means of the so-called target transformation, it can be determined whether a certain reference compound is suited for the modeling of the experimental data; that is, the model compounds that are required for a proper reproduction of the experimental data by means of a linear combination can be easily determined using PCA. This is especially interesting for the investigation of mixtures where the absorbing atom is present in several different phases as in the present case. PCA is equivalent to the methods in linear algebra, which are performed to determine the dimensionality of the vector space for the spectra. It is a commonly used tool, e.g., for spectroscopic techniques such as mass spectroscopy, infrared spectroscopy, Auger-electron spectroscopy, or UV−vis spectroscopy (see, e.g., refs 38−40), and has recently been applied also for the detailed analysis of X-ray absorption spectroscopy data.[36,37] The fraction with which the reference compounds are included in the reproduction of the individual spectra is determined by an associated weighting factor. This way, a detailed analysis of XANES and EXAFS is possible.

For evaluation of the reflection mode spectra, a linear preedge background $R_0(E)$ was fitted to the experimental data, interpolated to the postedge region and the normalized difference $R_0(E) - R(E)$ was calculated. The absorption edges (first inflection point) of these spectra were compared to those of reference compounds in order to obtain information about the average oxidation state of the Ti absorber. Since a straightforward interpretation of reflection mode spectra is not possible for layered systems due to the varying contributions of different layers as a function of the grazing angle, we calculated reflection

mode spectra for the analysis of the experimental spectra by means of the following procedures. Since the knowledge of both, the real (δ) and the imaginary part (β) of the complex index of refraction $n = 1 - \delta - i\beta$ is essential for the calculation of the X-ray reflectivity, we extracted the value of n from transmission mode EXAFS spectra by means of a Kramers−Kronig transform (see, e.g., refs 41 and 42). Assuming a multilayered structure consisting, e.g., of a thin layer of $Li_{0.6}TiO_2$ and an anatase film on top of a gold layer and the Si substrate, energy dependent Fresnel reflectivities were calculated[33] for different thicknesses of the individual layers in order to achieve a close fit to the experimental data.

2.3. In Situ Electrochemistry and Reflection Mode XAS. All electrochemical preparations were performed using the three-electrode electrochemical arrangement with copper counter and reference electrodes. The electrolyte solution consisted of 1 M $LiClO_4$ in propylene-carbonate (PC). The potential was controlled by an Eco Chemie Autolab PGSTAT30 potentiostat. Lithium was potentiostatically inserted (intercalation potentials between −1.5 and −2.1 V vs Cu, intercalation time between 20 min and 2 h) and extracted galvanostatically. All samples were measured under several glancing angles in order to vary the depth sensitivity of the X-ray experiments.

The main idea of the quasi-in-situ cell design is to remove the electrolyte from the sample surface after the electrochemical preparation and prior to the X-ray experiments in order to overcome the strong parasitic absorption of X-rays around the Ti K edge.[43] The cell is filled with inert He-gas, which continuously flushes through the cell during the experiments. Thereby, possible chemical reactions at the sensitive electrode and electrolyte materials are suppressed, and at the same time, the use of He gas also minimizes the parasitic absorption inside the cell.

3. Results and Discussion

3.1. Transmission XAFS. Upon lithiation, distinct changes are observed in the Fourier transform of the extended X-ray absorption fine structure, similar to what is reported, e.g., by ref 24. This is the result of the phase transition that takes place during the lithium insertion.[6] For compositions with $x > 0.5$, the structural changes in the EXAFS region are in agreement with diffraction results,[6,10] which have been previously reported in the XAS study by Luca et al.[24] In contrast to this study,[24] we treat the XAS data as originating from a two phases system, which appears to be the correct interpretation for average compositions roughly between $x = 0.01$ and 0.6.[8,10,14] The validity of the two-phase interpretation is investigated by a PCA analysis of the data. Indeed, PCA indicates the presence of only two contributing components, in this case the experimental spectra for Li_xTiO_2 $x = 0$ and 0.6. The XANES data can therefore be fitted with the combination of these two coexisting phases, anatase TiO_2 and Li-titanate ($Li_{0.6}TiO_2$). It should be mentioned here that after intercalation, a small fraction of Li ($x \approx 0.01$) is generally present in the anatase phase which is in equilibrium with the Li-rich Li-titanate phase.[9,10] The influence of this small amount of Li in the anatase on the resulting anatase X-ray absorption spectrum is assumed to be negligible. The PCA analysis and the least-squares fits are always performed for the normalized near edge X-ray absorption spectra $\mu(E)$. The fit residue is typically below 2−3%; that is, the fit quality is fairly good. A typical example obtained for $x = 0.32$ is presented in Figure 1a.

In addition, the application of PCA on the measured EXAFS spectra also indicates the presence of only two contributions.

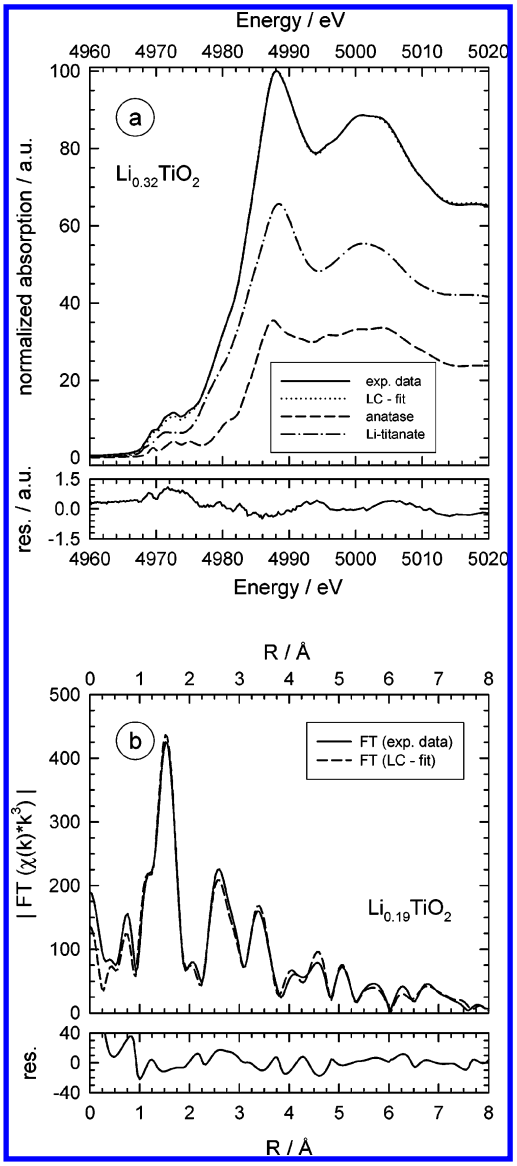

Figure 1. (a) Linear superposition of anatase and Li-titanate normalized XANES spectra $\mu(E)$ for a chemically intercalated Li_xTiO_2 sample with $x = 0.32$. The residual between the experimental data and the fit is shown in the lower part of this figure in the same units, with a maximum deviation smaller than 1.5%. (b) Magnitude of the Fourier transform of the k^3-weighted EXAFS data of a $Li_{0.19}TiO_2$ sample. Comparison of the experimental data to a linear combination (LC) fit. Again, the deviation between the fit and the experimental data is shown in the lower part of this figure in the same units. The data are not normalized and not corrected for phase shifts (Hanning windows, *k*-range for the FT: 2.5 Å^{-1} ≤ k ≤ 13.3 Å^{-1}).

Again, anatase TiO_2 and Li-titanate appear to be suitable reference compounds and the EXAFS data are fitted accordingly. An example is presented in Figure 1b in *R*-space representation. It has to be mentioned that the PCA analysis and the linear combination (LC) fits are performed with the k^3-weighted extended X-ray absorption fine structures $\chi(k)*k^3$ in the *k* range between 2.5 and 13.3 Å^{-1}. Subsequently, the experimental and the fitted $\chi(k)*k^3$ data are subjected to the Fourier transform. Fit residuals *R* were calculated from the difference between the experimental and calculated $\chi(k)*k^3$ and normalized to the experimental data in k-space; typical values amount to about $R \approx 2.28\%$. Again, the fit quality is excellent.

In summary, the observed changes in the fine structure of the EXAFS spectrum upon lithiation for all the investigated samples can be modeled using only different fractions of the

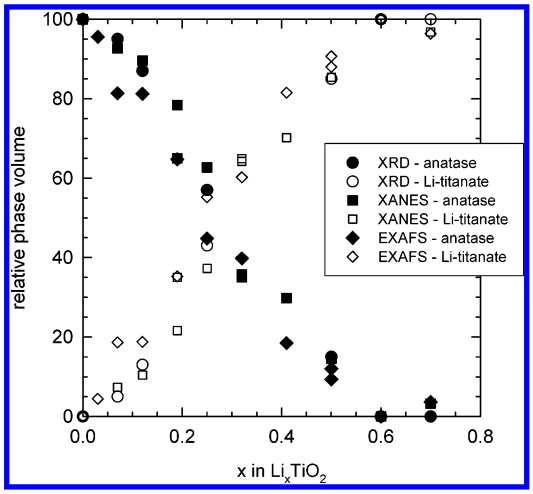

Figure 2. Relative phase volume of Li-anatase (Li_x~$0.01TiO_2$) and Li-titanate (Li_x~$0.6TiO_2$) resulting from the XANES and EXAFS least-squares fits of samples with compositions $0 \le x \le 0.7$. For comparison, XRD results from ref 9 are included.

anatase TiO_2 and Li-titanate spectra, the results of which are compiled in Figure 2. We assume these fractions to be the crystalline phase volume fractions and compare these with X-ray diffraction results; the latter were obtained in a previous study.[14] The XANES spectra of Li-titanate and pure anatase TiO_2 are shown in Figure 3a. In general, with increasing Li insertion ratio x, the preedge features labeled A_1 - A_3 and B, decrease in intensity while their positions remain nearly unchanged up to about $x = 0.3$. The edge positions, given by the first maximum of the derivative spectra, are shown in Figure 3b as a function of the insertion ratio. Since PCA gives strong evidence for the presence of only two principal components, the observed edge shifts with increasing x in Li_xTiO_2, Figure 3b, should not be interpreted as a homogeneous change of the Ti environment but rather as the result of the change in the relative weight of both edges originating from the two different crystallographic phases. The relative contributions of Li-anatase and Li-titanate as determined from the PCA analysis of the XANES region are also plotted in Figure 2. In summary, XRD, EXAFS, and XANES give quantitatively the same results implying that no significant amount ($<2-3\%$) of amorphous phases contribute to the XAFS signal.

As a consequence of the two-phase interpretation only differences between the anatase and Li-titanate XANES spectra, which are shown in Figure 3a, need to be considered. The pure anatase TiO_2 near edge structure has been the subject of several theoretical and experimental studies.[24,44-47] Throughout these theoretical studies, the various features have been controversely debated. Here we adapt the assignment of the preedge features as suggested by Wu et al.,[47] who appear to describe the experimental XANES spectrum of anatase TiO_2 most completely. The A_1 and A_2 pre-peaks are due to transitions of the core electrons toward the t_{2g} nonbonding bands whereas A_3 is the result of the e_g antibonding band. The t_{2g} and e_g bands represent the components of the crystal-field split Ti-3d atomic orbitals (AOs) that are shifted relative to each other in energy as a result of the octahedral oxygen surrounding of titanium (t_{2g}: d_{xy}, d_{yz}, d_{zx} and e_g: $d_{x^2-y^2}$, d_{z^2}). The lowering of the local symmetry, starting from a regular TiO_6 octahedron to the anatase octahedron, causes the t_{2g} band to split into two bands: d_{xy} (A_1) and d_{yz}, d_{zx} (A_2).[26,47] The changes in the XANES region upon Li insertion were first reported by Luca et al.[24] They observed a decrease of mainly the A_1 and B features and a shift of the

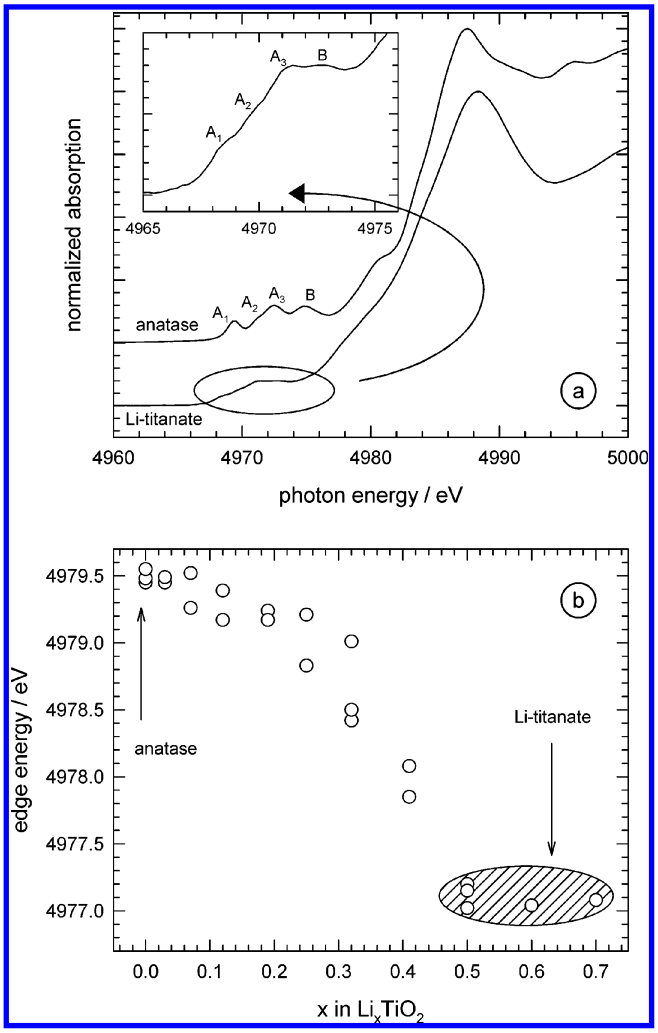

Figure 3. Near edge X-ray absorption (XANES) spectra of pure anatase TiO_2 and Li-titanate $Li_{0.6}TiO_2$ in the vicinity of the Ti K edge measured at room temperature. The preedge transitions A_1-A_3 and B are indicated for both spectra. In the inset, an enlarged view to the preedge peaks of Li-titanate is given. See text for more details. (b) Edge positions determined as the first inflection point of the EXAFS spectra of the powder samples with overall composition Li_xTiO_2 where x varies from 0 (pure anatase) to 0.7. Each data point corresponds to an independent sample preparation.

edge position and preedge features. These findings are confirmed by the present experimental results.

The interpretation of the changes in the XANES spectra is rather tedious since Li-ion intercalation not only leads to addition of electron density, but also leads to a phase transition into the Li-titanate structure.[6] However, the XANES transitions in anatase can, although strongly modified, still be distinguished in the Li-titanate spectrum, as can be seen in the inset of Figure 3a. In the next paragraphs, we attempt to explain the changes between the XANES spectrum of anatase and Li-titanate.

The edge position (the first inflection point of the absorption) shifts from the value of Ti^{4+} for anatase (4979.5 eV) toward 4977 eV for Li titanate. For comparison, Ti K edge energies of some selected Ti-reference compounds are given together with the formal Ti valence in Figure 4. As can be seen in this figure, a linear relation is well suited to describe the correlation between the oxidation state and edge positions of these Ti compounds, and lithium reduces the Ti valence-state in Li-titanate to about $Ti^{3.5+}$. Close inspection of the Li-titanate edge in Figure 3 shows that the edge extends over an energy range larger than the Ti K edge of pure anatase. For example, if the derivative spectra are

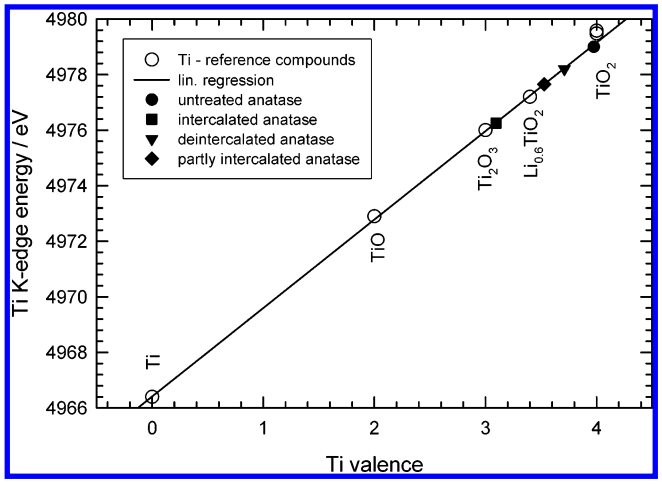

Figure 4. Edge position of various Ti compounds with different oxidation states. The straight line illustrates the linear relation between the oxidation state (valence) and the edge position. The edge position of the $Li_{0.6}TiO_2$ (Li-titanate) composition suggests an average Ti oxidation state of about 3.5+. In addition, also the Ti K edge positions determined from the reflection mode near edge spectra are indicated for the untreated, intercalated, partly intercalated, and deintercalated anatase samples.

TABLE 1: Fit Results for the A_1, A_2, A_3, and B Transitions in the XANES Region for Anatase and Li-Titanate

		E [eV]	fwhm [eV]	area
anatase	A_1	4969.42 ± 0.10	1.96 ± 0.20	16.2 ± 0.2
	A_2	4971.15 ± 0.10	1.21 ± 0.10	6.2 ± 0.2
	A_3	4972.39 ± 0.10	1.60 ± 0.05	14.5 ± 0.2
	B	4974.82 ± 0.10	3.20 ± 0.20	34.5 ± 0.5
Li-titanate	A_1	4968.59 ± 0.10	2.53 ± 0.20	10.9 ± 0.5
	A_2	4970.65 ± 0.10	2.10 ± 0.10	6.0 ± 0.2
	A_3	4971.36 ± 0.10	2.92 ± 0.05	9.1 ± 0.7
	B	4972.98 ± 0.10	3.07 ± 0.15	15.3 ± 1.0

considered, the width of the edge has increased from about 4.7 ± 0.2 eV for pure anatase to ca. 7.3 ± 0.2 eV for Li-titanate. Therefore, it seems likely that the oxidation-state of Li-titanate is not a homogeneous oxidation state of $Ti^{3.5+}$ but rather a distribution between Ti oxidation states, roughly between 4+ and 3+. It should be realized, however, that it is not trivial to determine the oxidation state from the edge position, since the atomic structure in Li-titanate is different from anatase. In addition to the influence of the oxidation state, changes in bond distances will also shift the XANES transitions. For example, the white line feature (the most intense peak in the XANES region of the spectrum), which corresponds to transitions of the photoelectron into unoccupied states above the Fermi level, shifts from about 4987.5 eV in anatase to about 4988.5 eV in Li-titanate. However, this shift agrees qualitatively with the increasing antibonding character of this transition and the decreasing Ti−O distances in Li-titanate. In addition, for several different Mo compounds with different ligands, a linear relation between the charge on the absorbing Mo ion and the position of the first inflection point has been established.[48] Therefore, the oxidation state, as determined here with respect to reference compounds, should be treated as a rough estimate.

Fitting the preedge features, assigned A to B results in the intensities and shifts listed in Table 1. Comparing the preedge features between Li-titanate and anatase reveals clear changes in energy position and intensity. The A_1 transition has largely disappeared but has a relatively small change in transition energy. The distinct decrease in intensity of the A_1 transition indicates that Li ion intercalation reduces the transition probability toward the t_{2g} band. This can be explained by occupation of this band by the charge-compensating electrons, in agreement with what is generally accepted, and more specifically predicted by ab initio calculations.[26] It should however be realized that these bands have a strong O-2p admixture.[17] The transition probability, i.e., the intensity of the prepeaks, is also in another way related to the structure. Changes in the structure lead to modification of the p-character of the unoccupied states. Due to the phase transition from anatase toward Li-titanate, the TiO_6 octahedrons become more regular,[6] which will reduce the transition probabilities. This explains why all the transitions are reduced in intensity, whereas occupation of the lowest unoccupied t_{2g} bands by charge compensating electrons only reduces the A_1 transition.

In principle, the t_{2g} bands have a nonbonding character; however, the reduction in symmetry due to the phase transition from the anatase toward the Li-titanate structure predicts that the d_{yz} component becomes bonding and shifts down in energy toward the d_{xy} component.[26] This is actually argued to be the origin of the phase transition, as the occupation of these binding d_{yz} bands reduces the Ti−Ti distances in *yz* direction causing the formation of Ti−Ti zigzag chains in this direction.[6,26] The d_{xy} band remains nonbonding, whereas the d_{zx} component becomes antibonding.[26] The observed reduction of the A_2 transition intensity is consistent with the previous argumentation, the A_2 transition loses the d_{yz} band to the A_1 transition, although it is likely additionally the result of the more regular TiO_6 octahedrons in Li-titanate as discussed above. The antibonding character of the d_{xz} band explains the shift of the A_2 transition to lower energies because the distance of Ti−Ti neighbors in the *zx* direction increases, thereby reducing the electron overlap. In addition the reduction of the Ti−Ti distances in the *yz* direction causes the A_1 transition to widen, in agreement with what is observed. The shift toward lower energies of the A_3 transition is consistent with the Ti−O bond length changes and the antibonding character of the e_g band. Lithiation of anatase causes the Ti−O bond length to increase in Li-titanate leading to a smaller σ overlap between the T-3d and O-2p orbitals. The shift and decrease of the *B* transition can be ascribed to the antibonding character of the Ti-4p,Ti-4s, and/or O-2p hybridized bands and more regular TiO_6 octahedrons in Li-titanate, respectively. The same arguments apply for the higher located transitions which are associated with the antibonding Ti-4p, O-2p bands.

Optical absorption of Li-titanate leads to two broad absorption peaks located at 390 nm (3.18 eV) and 700 nm (1.77 eV).[21] Based on the assignment of the present XANES transitions, the optical transitions are likely the result of transitions from localized electrons (see below) at the bottom of the t_{2g} band (A_1 transition) toward the upper part of the t_{2g} band (A_2) and the e_g band (A_3). These broad, but well-defined, optical absorption peaks are in contrast to the typical free electron absorption characteristics of anatase during the initial stage of the intercalation process (double layer regime).[21]

The notion that the increased edge width of Li-titanate is most likely the result of a distribution of oxidation states does not agree with a nearly free electron picture[18,19] where the delocalized band character can be expected to lead to a more homogeneously distributed Ti valence resulting in a well defined edge position. In a more localized electron picture, the distribution of possible valences may be explained by the local random Li occupation of sites. Note that only half of the oxygen octahedrons are occupied with a Li-ion and this Li may be on two different crystallographic positions.[10] A more localized electron state character is also suggested by broad optical

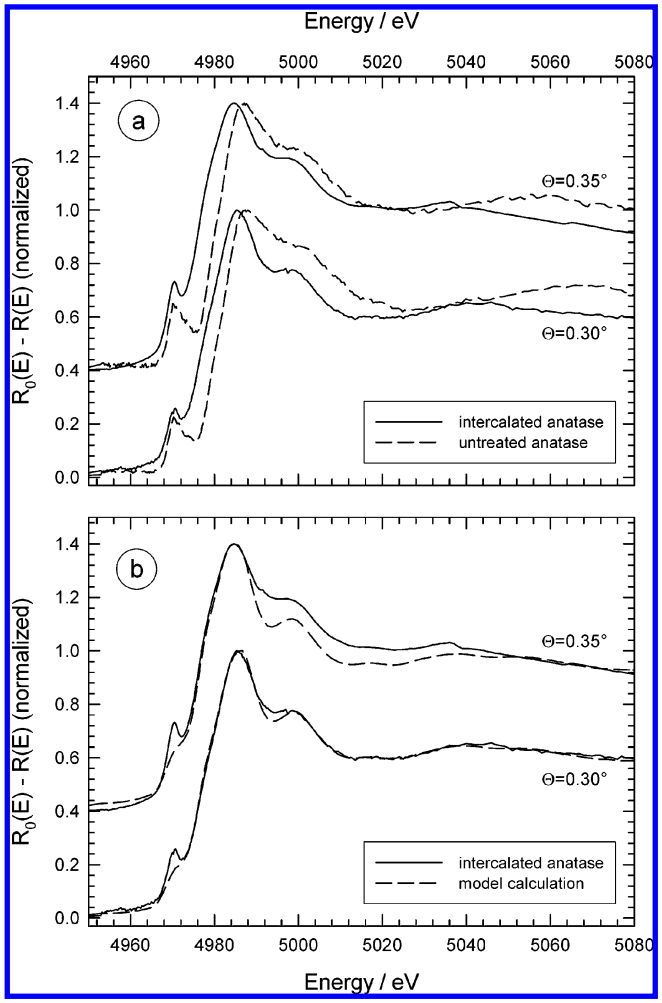

Figure 5. (a) Comparison of the experimental normalized XANES spectra $R_0(E) - R(E)$ determined from reflection mode spectra for an intercalated (full line) and the untreated (dashed line) anatase electrode for two glancing angles. $R_0(E)$ denotes a linear preedge background, fitted to the data below 4950 eV. Approximate penetration depths for glancing angles θ=0.30° and 0.35° are 4 and 5−10 nm, respectively. (b) Comparison of the XANES data determined form the measured near edge reflection mode spectra (full lines) and calculated spectra (dashed lines) assuming a multilayered structure consisting of a top layer of 4 nm Ti_2O_3 on 25 nm Li-titanate on an underlying gold backing electrode (10 nm) on the Si substrate. No anatase contributions are needed to fit the data. (The spectra are shifted vertically by 0.4 units for $\Theta = 0.35°$ for a better comparison).

absorption bands[21] and the nonmetallic conductivity.[20,21] Finally, the localized character is suggested by the formation of Ti−Ti zigzag bonds in the *yz* direction as can be explained by filling of the bottom of the conduction band consisting of Ti-3d_{yz} orbitals (part of the t_{2g} band),[26] which is consistent with the present XANES spectra. These localized bonding orbitals imply a covalent character[20] that is often observed in combination with the disappearance of magnetic moments (quenching of the orbital momentum).[49] If in addition there is no profound polarization of the electron spin states, the covalent character also explains the absence of a significant amount of paramagnetic Ti^{3+} states as is concluded from NMR experiments.[14,24]

3.2. XAFS in Reflection Mode. For intercalated anatase TiO_2, Figure 5, the reflection mode spectra at different glancing angles indicate that the complete, approximately 25 nm thick, anatase layer is modified by the Li intercalation. For the largest glancing angle measured, $\Theta = 0.40°$ (not shown in Figure 5) with a penetration depth of more than 50 nm, the spectrum is recognized as that of Li-titanate: Although the spectrum is strongly distorted by the effect of the anomalous dispersion, the observed minima and maxima in the derivative absorption spectrum correspond well to those of the Li-titanate reference compound measured in transmission. Moreover, the corresponding edge position leads to a Ti oxidation state of +3.4, which is comparable to that of the bulk Li-titanate, +3.5, found with XANES in transmission mode. The changes in the preedge region upon intercalation going from anatase to Li-titanate are similar to those measured with transmission XAFS; that is, in the Li-titanate phase, the Ti-3d t_{2g} band located at the bottom of the conduction band is partially occupied by the charge compensating electrons, as is discussed above.

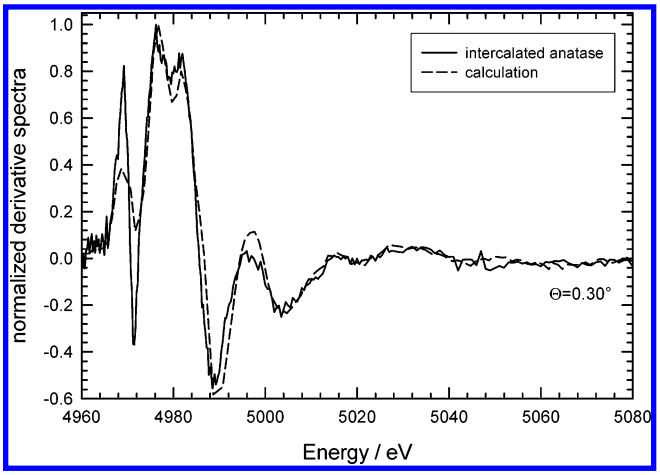

Figure 6. Comparison of the derivative near edge X-ray absorption spectrum measured for a fully intercalated anatase sample at $\Theta = 0.30°$ (full line) to a model calculation (dashed line) for a multilayered system consisting of a top layer of 4 nm Ti_2O_3 on 25 nm Li-titanate on an underlying gold backing electrode (10 nm) on the Si substrate.

At $\Theta = 0.30°$, with a penetration depth of about 3−4 nm, the edge shift is more pronounced compared to the untreated film, and comparing the edge position with the reference data in Figure 4, the Ti oxidation state results in a value close to +3. For a more detailed analysis of the reflection mode XANES spectra of the fully intercalated state, we simulated spectra for multilayered specimen with different individual layer thicknesses and compositions. Various Li-containing Ti-oxide compounds such as the Li-spinel $Li_4Ti_5O_{12}$ and Li-titanate ($Li{\sim}0.6TiO_2$) were tested, but the best fit of the experimental XANES data was obtained for a model structure consisting of a thin Ti_2O_3-oxide layer on top of the Li-titanate phase (see Figure 5b). Our calculations suggest a thickness of the Ti^{3+} oxide of about 4 nm. To stress our findings, we compared the derivative of the experimental data and the model calculation in Figure 6. Besides the intensity of the preedge peak at about 4970 eV, all peak positions and intensities are well reproduced by the model calculation. This indicates that a thin Ti^{3+} layer, with a XANES structure similar to that of Ti_2O_3 is formed on a Li-titanate layer by the electrochemical intercalation of anatase TiO_2.

After the first intercalation/deintercalation cycle, the Ti^{3+} top layer is also present in the partly charged and deintercalated state, although the thickness is reduced to a few angstroms. This is shown in Figure 7 for the XANES data measured after deintercalation and a subsequent partial charging to ca. 50% of the maximum charge. The experimental data are compared to a fit with a multilayered structure consisting of a 0.4 nm thick Ti_2O_3 film on top of a Li-titanate film (20 nm thickness), a 10 nm anatase TiO_2 film, and the gold contact layer. Both the XANES spectra and their derivatives are compared. Although several smaller deviations between the calculated and the measured data can be seen, for example, the calculations always

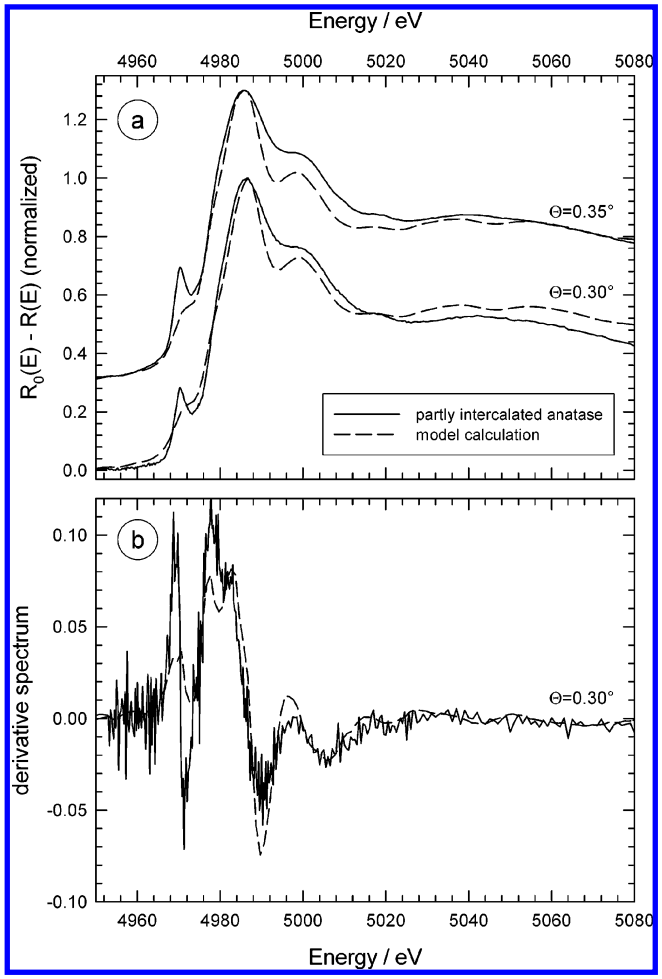

Figure 7. Fit of the near edge X-ray absorption spectra measured for a partly intercalated anatase electrode (full lines) with a model structure (dashed lines) consisting of 0.4 nm Ti_2O_3 film on top of a Li-titanate film (20 nm thickness), 10 nm anatase TiO_2 and the gold contact layer on top of the Si substrate. (a) Normalized absorption spectra, (b) derivative spectra.

TABLE 2: Composition of the Multilayered Structure that Was Formed in Thin Film Anatase Working Electrodes in 1 M $LiClO_4$ + PC after Full Electrochemical Intercalation, after Partly Intercalation, and after Deintercalation[a]

	layer thickness (nm)			
	Ti_2O_3	$Li_{0.6}TiO_2$	anatase TiO_2	Au contact
fully intercalated anatase	4.0	25.0		10.0
deintercalated anatase		6.0	23.0	10.0
partly intercalated anatase	0.4	20.0	10.0	10.0

[a] The given thickness values were derived from a detailed modeling of the reflection mode near edge spectra of the anatase samples after the different electrochemical treatments.

suggest a less pronounced hump in the XANES spectra at about 4995 eV, the overall agreement between simulated and measured data is reasonable, especially with regard to the huge problems which generally occur when measured XANES-spectra of inhomogeneous sample systems are fitted using model calculations (compare, e.g., ref 46). Most of the positions and intensities of the pre- and postedge features are well reproduced by the calculations also in the derivative spectra, and thus the similarity of the measured and calculated spectra appears acceptable. The measured spectra were best fitted by the thickness values for the Ti^{3+}, $Ti^{3.5+}$, and Ti^{4+} layers given in Table 2. Apparently, the transformation toward the Li-containing Ti-oxide material

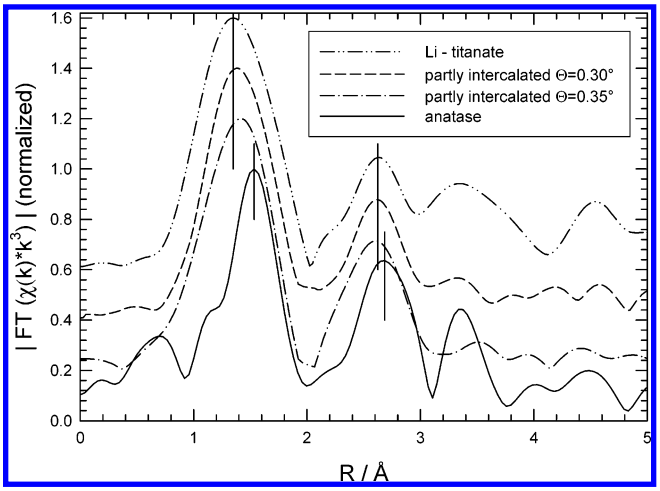

Figure 8. Comparison of the normalized magnitude of Fourier transforms of the experimental transmission mode spectra of anatase and Li-titanate ($Li_{0.6}TiO_2$) to those calculated from reflection mode spectra of partly intercalated anatase samples after a completed charge/discharge cycle. Vertical bars indicate the peak positions corresponding to the first two coordination shells of anatase and Li-titanate. (The data are not phase-shift corrected. Hanning windows, K range for the FT: 2.5 $Å^{-1} \leq k \leq 13.3\ Å^{-1}$.)

which resembles the XANES of Ti_2O_3 is not completely reversible, and after the first cycle, a few angstroms remain present.

The near neighbor atomic configuration is probed with the EXAFS part of the reflection mode spectra. As an example, we present in Figure 8 the Fourier transforms of a partly intercalated anatase electrode together with the transmission EXAFS result of anatase TiO_2 and Li-titanate. The nearest neighbor peak of the partly intercalated sample at 1.4 Å is very similar to that of Li-titanate in position and half width for $\Theta = 0.30°$, whereas the second nearest neighbor peak has larger intensity compared to the Li-titanate but is smaller than pure anatase. For $\Theta = 0.35°$ the first peak shifts to a larger radial distance and the half width becomes smaller. The intensity of the second nearest neighbor peak increases with grazing angle; that is, it becomes more similar to anatase. In agreement with model calculations, the thickness of the Ti^{3+} layer is too small to result in detectable changes of the measured EXAFS fine structures. The structure of the partly intercalated electrode is thus given by a layered system with Li-titanate on top of the anatase and the refinement of the measured XANES data indicates the presence of a very thin Ti^{3+} layer on top of this duplex layer (see Figure 7).

The EXAFS signal of the fully intercalated anatase for $\Theta = 0.30°$ material is compared with that of Li-titanate and Ti_2O_3, both displayed in Figure 9. Both the intensities and the positions of the first two coordination shells of the measured reflection mode spectrum are almost identical to those of the Li-titanate. From this comparison, it is clear that the near neighbor atomic configuration of the first 4 nm, characterized by Ti^{3+} states, is comparable with that of the Li-titanate phase. Therefore, it is concluded that Li intercalation into anatase TiO_2 leads to the transformation toward the Li-titanate material, and on top of that, a thin film of ~4 nm thickness has a similar atomic structure compared to Li-titanate but with a Ti valence close to 3+ (as in Ti_2O_3). The effective Ti^{3+} valence of the top layer suggests a composition close to Li_1TiO_2 in order to preserve local charge neutrality. Assuming a similar crystallographic structure as Li-titanate, it seems reasonable that in Li_1TiO_2 all of the available octahedral sites will be occupied by Li, whereas in the Li-titanate, every second site remains unoccupied.[6] Note

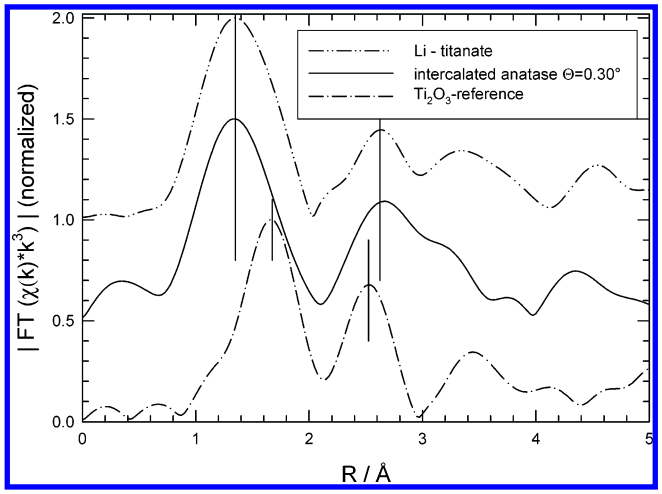

Figure 9. Comparison of the normalized magnitudes of Fourier transforms of the experimental transmission mode spectra of Ti_2O_3 and Li-titanate ($Li_{0.6}TiO_2$) to those calculated from a reflection mode spectrum of a fully intercalated anatase sample. Vertical bars indicate the peak positions corresponding to the first two coordination shells of Ti_2O_3 and Li-titanate. (The data are not phase-shift corrected. Hanning windows, *K* range for the FT: 2.5 $Å^{-1} \leq k \leq 13.3$ $Å^{-1}$.)

that the thickness of the layer is such that the charge cannot be compensated by ions absorbed at the surface, and additional Li ions are required to intercalate into the material for charge compensation.

Fourier transforms of the deintercalated electrode (not shown) show strong contributions of anatase for all glancing angles. However, there are clear indications for remaining Li-titanate in these spectra, i.e., a broadened nearest neighbor peak at about 1.4 Å radial distance and a significantly reduced intensity of the second coordination shell at ca. 2.6 Å. This also supports the XANES data analysis for this sample, which predicts a remaining Li-titanate layer with a thickness of about 6 nm after deintercalation (see Table 2).

Studies with XPS and L edge XAFS using soft X-rays, yielding information on the first ~4 nm of a nanoporous sample, characterize Li-intercalated anatase with a considerable amount of Ti^{3+} states in addition to Ti^{4+} states.[7,22] In contrast to that, the XANES in reflection mode shown in the present study indicates that, fully intercalated, the first ~4 nm is characterized by an effective Ti oxidation state 3+, in contrast to a distribution of 4+ and 3+ states. This controversy might be resolved by considering differences in sample morphology, and related overall composition of the intercalated films. Henningson et al. report a maximum insertion ratio $x = 0.4$ for nanoporous anatase TiO_2.[7] The present thin film material appears to be intercalated up to x ~ 0.6 (as judged from the average Ti oxidation state of the Li-titanate phase) and even higher for the top layer. Apparently, the present electrochemical insertion of the thin film anatase TiO_2 material leads to a higher insertion capacity compared to experiments presented by Henningson et al.[7] In this context, literature indicates that the maximum intercalated charge in anatase TiO_2 strongly depends on the exact sample morphology and environment − i.e., the long as well as the short range order structure plays an essential role (see also[50]). In addition to $x = 0.4$ reported by Henningson et al. for nanoporous material,[7] electrochemical insertion is also reported to result in $x = 0.5$ for poly-crystalline thin films[8] and nanoporous anatase.[27] For nano-crystalline anatase, insertion ratios above 0.5 have been reported,[9] and at elevated temperatures values up to $x = 1$ were found for microscopically porous materials,[12] whereas chemical lithiation generally leads to a maximum value around 0.6−0.7.[11] Clearly, the microstructure influences the insertion capacity, and more specifically, Fattakhova et al. illustrated that there might even be an optimal crystallite dimension (~100 nm) to achieve the highest insertion capacity.[51] In view of previous studies, it is not unlikely that the inserted charge in the present study exceeds $x = 0.4$. Therefore, it is proposed that the additional layer presently found is a new Li-titanate like phase with a Ti oxidation state close to 3+ and a composition Li_1TiO_2, which is not observed for compositions with $x < 0.5$.

It is interesting to compare these results with the intercalation at elevated temperatures by Macklin et al.,[12] who reported a second constant potential plateau in the discharge curves (constant current setting) at x ≈ 0.6, indicating the formation of a new phase with composition Li_1TiO_2. From the similarity of the discharge curve and based on X-ray diffraction at the composition $x = 0.7$, Macklin et al. concluded that the material retained its original structure, i.e., the Li-titanate structure. In qualitative agreement with that, the present surface sensitive EXAFS indicates the presence of the Li_1TiO_2 phase, with an atomic short-range order configuration similar to Li-titanate. Here, the formation of this Li_1TiO_2 material is limited to a thin surface layer at room temperature, whereas at 120 °C, the whole material will be converted to composition $x = 1$, as is illustrated by the results of Macklin et al. In this context, additional surface sensitive X-ray absorption studies at elevated temperatures are highly desirable. The cycle ability at elevated temperatures after the formation of the Li_1TiO_2 material is worse compared to the cycle ability up to a maximum composition $x = 0.5$.[12] This might indicate that the formation of the $x = 1$ material fractures the anatase TiO_2 electrode material in such a way that it leads to a decrease of the capacity within a few cycles.

The present results indicate that Li-intercalation proceeds as a plane front Li-titanate that transforms the original anatase structure, in agreement with a recent neutron reflectometry study on Li intercalation in anatase TiO_2 films, where the Li-titanate phase front could be observed in-situ during insertion and extraction.[13] The additional layer detected with XAFS in reflection mode was not directly observed with neutron reflectometry, possibly because of the lack of scattering contrast with the Li-titanate phase and the limited layer thickness.

The observation of a ~4 nm thin surface layer characterized by an effective Ti^{3+} oxidation state is new and suggests a composition close to Li_1TiO_2, a composition that has only reported at elevated temperatures.[12] The underlying Li-titanate phase, composition $Li{\sim}0.6TiO_2$, has an average oxidation state of 3.4+, and similar XANES and EXAFS spectra compared to the transmission experiments that probe the bulk Li-titanate properties. The prominent difference between the bulk and the surface properties is the ~4 nm surface layer. The influence of this layer on the electro-chromic properties remains unclear so far. This study reveals that the surface oxidation state is close to 3+ and that the near neighbor atomic structure is similar to that of Li-titanate. Further research will be necessary to determine the exact properties of this surface layer and its influence of the electro-chromic properties of lithiated anatase.

4. Conclusions

A two phase system is completely suited to explain the changes in the EXAFS and XANES regions of the X-ray absorption spectra of anatase TiO_2 upon Li intercalation. This finding is in accordance with our previous structural studies with XRD and NMR. The changes in the near K edge region of Ti indicate that the electron density, donated by the inserted

Li, occupies the bonding part of the crystal field split Ti-3d t_{2g} Ti−Ti orbitals positioned at the bottom of the conduction band as has been predicted by Lunell et al.[26] The distribution in the Ti edge position, observed in Li-titanate, indicates a distribution of Ti valences around $Ti^{3.5+}$.

Quasi in situ reflection mode EXAFS experiments at the Ti K edge of Li intercalated anatase TiO_2 electrodes indicate structural changes of the electrode surface structure as well as changes of the electronic state of the absorbing Ti atoms. The anatase TiO_2 film of about 25 nm thickness appears to be completely intercalated forming the $Li_{x\sim0.6}TiO_2$ phase with an average oxidation state of about +3.4. Of particular interest is the Ti K edge shift at the surface region of the anatase, which is interpreted by the existence of Ti^{3+} states, suggesting a material with composition close to Li_1TiO_2. Comparison of the experimental data with model calculations suggests a thickness of this Ti^{3+} layer of about 4 nm after full intercalation. The crystallographic structure appears to be similar to that of the Li-titanate structure. The layer appears to fracture the electrode surface leading to a decrease of Li capacity during following (dis)charge cycles. Further research is necessary to establish details of the charge cycling and the electro-chromic properties of this surface layer compared that of the Li-titanate phase.

Acknowledgment. The thin film anatase TiO_2 samples were prepared by D. Blank and F. Roesthuis of the Material Science group, Department of Applied Physics, University of Twente, The Netherlands. We like to thank HASYLAB and the MWF Nordrhein-Westfalen for the support of our experiments. This work was supported by the IHP-Contract HPRI-CT-1999-00040 of the European Community.

References and Notes

(1) Bonino, F.; Busani, L.; Manstretta, M.; Rivolta, B.; Scrosati, V. *J. Power Sources* **1981**, *6*, 261.
(2) Huang, S. Y.; Kavan, L.; Exnar, I.; Grätzel, M. *J. Electrochem. Soc.* **1995**, *142*, L142.
(3) Ohzuku, T.; Takehara, Z.; Yoshizawa, S. *Electrochim. Acta* **1979**, *24*, 219.
(4) Ohzuku, T.; Hirai, T. *Electrochim. Acta* **1982**, *27*, 1263.
(5) Bechinger, C.; Ferrere, S.; Zaban, A.; Sprague, J.; Gregg, B. *Nature* **1996**, *383*, 608.
(6) Cava, R. J.; Murphy, D. W.; Zahurak, S.; Santoro, A.; Roth, R. S. *J. Solid State Chem.* **1984**, *53*, 64.
(7) Henningsson, A.; Rensmo, H.; Sandell, A.; Siegbahn, H.; Södergren, S.; Lindström, H.; Hagfeldt, A. *J. Chem. Phys.* **2003**, *118*, 5607.
(8) *J. Phys. Chem. B* **1999**, *103*, 7151.
(9) Krtil, P.; Fattakhova, D.; Kavan, L.; Burnside, S.; Grätzel, M. *Solid State Ionics* **2000**, *135*, 101.
(10) Wagemaker, M.; Kearley, G. J.; van Well, A. A.; Mutka, H.; Mulder, F. M. *J. Am. Chem. Soc.* **2003**, *125*, 840.
(11) Wittingham, M. S.; Dines, M. B. *J. Electrochem. Soc.* **1977**, *124*, 1387.
(12) Maclin, W. J.; Neat, R. J. *Solid State Ionics* **1992**, *53*−*56*, 694.
(13) Wagemaker, M.; van de Krol, van Well, A. A. *Physica B* **2003**, *336*, 124.
(14) Wagemaker, M.; van de Krol, R.; Kentgens, A. P. M.; van Well, A. A.; Mulder, F. M. *J. Am. Chem. Soc.* **2001**, *123*, 11454.
(15) Wagemaker, M.; Kentgens, A. P. M.; Mulder, F. M. *Nature* **2002**, *418*, 397.
(16) Bruce, P. G. *Solid State Electrochemistry*. Cambridge University Press: Cambridge, 1995.
(17) Aydinol, M. K.; Kohan, A. F.; Ceder, G.; Cho, K.; Joannopoulos, J. *Phys. Rev. B* **1997**, *56*, 1354.
(18) Enright, B.; Fitzmaurice, D. *J. Phys. Chem.* **1996**, *100*, 1027.
(19) Kavan, L.; Grätzel, M.; Rathousky, J.; Zukal, A. *J. Electrochem. Soc.* **1996**, *143*, 394.
(20) Murphy, D. W.; Greenblatt, M.; Zahurak, S. M.; Cava, R. J.; Waszczak, J. V.; Hull, G. W.; Hutton, R. S. *Rev. Chim. Miner.* **1982**, *19*, 441.
(21) van de Krol, R.; Goossens, A.; Meulenkamp, E. A. *J. App. Phys.* **2001**, *90*, 2235.
(22) Södergren, S.; Siegbahn, H.; Rensmo, H.; Lindström, J.; Hagfeldt, A.; Lindquist, S. E. *J. Phys. Chem. B* **1997**, *101*, 3087.
(23) Cao, F.; Oskam, G.; Searson, P. C.; Stipkala, J. M.; Heimer, T. A.; Farzad, F.; Meyer, G. J. *J. Phys. Chem.* **1995**, *99*, 11974.
(24) Luca, V.; Hanley, T. L.; Roberts, N. K.; Howe, R. F. *Chem. Mater.* **1999**, *11*, 2089.
(25) Luca, V.; Hunter, B.; Moubaraki, B.; Murray, K. S. *Chem. Mater.* **2001**, *13*, 796.
(26) Nuspl, G.; Yoshizawa, K.; Yamabe, T. *J. Mater. Chem.* **1997**, *7*, 2529.
(27) van de Krol, R.; Goossens, A.; Meulenkamp, E. A. *J. Electrochem. Soc.* **1999**, *146*, 3150.
(28) Pizzini, S.; Roberts, K. J.; Greaves, G. N.; Harris, N.; Moore, P.; Pantos, E.; Oldman, R. J. *Rev. Sci. Instrum.* **1989**, *60*, 2525.
(29) Bosio, L.; Cortes, R.; Delichere, P.; Froment, M.; Joiret, S. *Surf. Interface Anal.* **1988**, *12*, 380.
(30) Borthen, P.; Strehblow, H.-H. *Phys. Rev. B* **1995**, *52*, 3017.
(31) Hecht, D.; Frahm, R.; Strehblow, H.-H. *J. Phys. Chem.* **1996**, *100*, 10831.
(32) Lützenkirchen-Hecht, D.; Frahm, R. *Physica B* **2000**, *283*, 108.
(33) Parratt, L. G. *Phys. Rev.* **1954**, *95*, 359.
(34) Frahm, R.; Weigelt, J.; Meyer, G.; Materlik, G. *Rev. Sci. Instrum.* **1995**, *66*, 1677.
(35) Ressler, T. *J. Synchrotron Rad.* **1998**, *5*, 118. See also: www-.winxas.de
(36) Wasserman, S. R. *J. Phys. IV (France)* **1997**, *7*, C2−203.
(37) Ressler, T.; Wong, J.; Roos, J.; Smith, I. L. *Environ. Sci. Technol.* **2000**, *34*, 950.
(38) Jackson, J. E. *A user's guide to principal components*; John Wiley & Sons: New York, 1991.
(39) Malinowski, E. R.; Howery, D. G. *Factor analysis in chemistry*; John Wiley & Sons: New York, 1980.
(40) van Lier, J.; Baretzki, B.; Zalar, A.; Mittemeijer, E. J. *Surf. Interface Anal.* **2000**, *30*, 124.
(41) Borthen, P.; Strehblow, H.-H. *Physica B* **1995**, *208&209*, 421.
(42) J. O. Cross, J. O.; Newville, M.; Rehr, J. J.; Sorensen, L. B.; Bouldin, C. E.; Watson, G.; Gouder, T.; Lander, G. H.; Bell, M. I. *Phys. Rev. B* **1998**, *58*, 11215.
(43) Lützenkirchen-Hecht, D.; Wagemaker, M.; Keil, P.; van Well, A. A.; Frahm, R. *Surf. Sci.* **2003**, *538*, 10.
(44) Grunes, L. A. *Phys. Rev. B* **1983**, *27*, 2111.
(45) Brydson, R.; Sauer, H.; Engel, W.; Thomas, J. M.; Zeitler, E.; Kosugi, N.; Kuroda, H. *J. Phys.: Condens. Matter* **1989**, *1*, 797.
(46) Ruiz-Lopez, M. F.; Munoz-Paez, A. *J. Phys.: Condens. Matter* **1991**, *3*, 8981.
(47) Wu, Z. Y.; Ouvrard, G.; Gressier, P.; Natoli, C. R. *Phys. Rev. B* **1997**, *55*, 10382.
(48) Cramer, S. P.; Eccles, T. K.; Kutzler, F. W.; Hodgson, K. O.; Mortenson, L. E. *J. Am. Chem. Soc.* **1976**, *98*, 1287.
(49) Cotton, F. A.; Wilkinson, G. *Advanced Inorganic Chemistry*; John Wiley and Sons: New York, 1972.
(50) Hibino, M.; Abe, K.; Mochizuki, M.; Miyayama, M. *J. Power Sources* **2004**, *126*, 139.
(51) Fattakhova, D.; Kavan, L.; Krtil, P. *J. Solid State Electrochem.* **2001**, *5*, 196.